

Synthesis and Properties of N-substituted Polyurethane Used in Leather

Finishing

Yanyan Wang, Libin Liu, Congde Qiao, Tiaoduo Li

Shandong Provincial Key Laboratory of Fine Chemicals, Key Laboratory of Fine Chemicals in Universities of Shandong, Shandong Polytechnic University, Jinan 250353, P. R. China

Correspondence to L. B. Liu (E-mail: lbliu@spu.edu.cn) or T. D. Li (E-mail: litianduo@163.com)

ABSTRACT: N-alkyl-substituted polyurethanes with different alkyl chain length were prepared from bromoalkane (1-Bromooctane, 1-Bromotetradecane, 1-Bromooctadecane), and polyurethane consisted of poly(propylene glycol), 4,4'-diphenylmethane diisocyanate, and 1,4-butanediol. The final materials were characterized by ¹HNMR and FTIR and their degree of substitutions were discussed by changing reaction conditions. DSC and XRD were used to characterize thermal properties and crystalline state. Microphase-separated nanostructure, with hard segments (nanofiber-like) embedded into an amorphous PPG soft segments are observed by AFM and SEM. Reversible behavior of the films was revealed by contact angle measurement. Stimuli-responsive films were realized by solvent vapor annealing experiment and heat treatment, which exhibited the reversible switching in its surface wettability with a remarkable change in the water contact angle of 21°.

KEYWORDS: N-alkyl-substituted polyurethanes; stimuli-responsive films; surface morphology; thermal properties; contact angle

INTRODUCTION

Responsive polymers, whose characteristics change in response to an external signal, such as temperature, pH, light, solvent, electric potential, or magnetic field,¹ are playing an increasingly important part in a diverse range of applications, such as drug delivery,^{2,3} diagnostics, analytical chemistry, biomedical engineering,⁴ tissue engineering and 'smart' optical systems, as well as biosensors,⁵ microelectromechanical systems, coatings⁶⁻⁹ and textiles.¹⁰ As a class of unique intelligent polymers, interest in polyurethane (PU) materials has been focused more extensively due to their favorable and controllable properties and they are extensively used in adhesives, thermoplastic elastomers, insulation, sealants, coatings and foams.¹¹⁻¹³ Polyurethanes can be easily prepared by simple polyaddition reaction of polyols, isocyanates and chain extenders.¹⁴ The polymeric materials have quite a wide spectrum of properties, depending upon the nature of the starting materials,¹⁵ so the properties of polyurethane materials can be regulated by the variation of their components. However the

wider use of PUs limited by the thermal degradation when thermoplastic processing at temperature above 200 °C,¹⁶ they are split back into starting polyols and isocyanates. The labile hydrogen of the carbamate group is primarily responsible for the thermal degradation of polyurethane.

Recently, many works on improvement in properties of polyurethane has been performed. One of the most powerful approaches is carried out by chemical modification of labile hydrogens of the carbamate replaced by halogenides after preliminary metalation of the polymer with sodium hydride under suitable condition.¹⁷⁻¹⁹ N-modification is mainly directed to improve typically desired properties of the materials, such as enhanced thermostability, fire retardancy, flexibility, solubility, and so forth.²⁰⁻²⁸ Improvements in these properties have more or less been achieved by grafting. For example, Kweon²⁵ and Choi²⁶ reported that the stabilization of PU is improved on N-substitution because that the replacement of the N-hydrogen by an alkyl group prevents back dissociation. S. M. Seyed Mohaghegh²⁷ investigated properties of polyurethane modified by N-substituted with poly(ethylene glycol monomethyl ether) which have great flexibility and increased hydrophilicity. Liaw and Lin²⁸ studied that the metalation and N-alkylation of phosphorus containing polyurethanes exhibiting enhanced fire resistance and increased solubility. Up to now, most of the research was carried out with the N-methylation of PU, and only a few limited studies have been reported on the N-substituted PU, especially PU with alkyl side chains longer than methyl.²⁵ Moreover, stimuli-responsive N-substituted PU films and the influence of N-modification of PU on surface topography have not been investigated so far.

The aim of the present work was to synthesize and characterize three kinds of N-alkyl-substituted PUs with various substituent. The idea degree of substitutions were gained through changing reaction conditions. The effect of N-substitution on the surface morphologies and thermal properties were studied. In addition, by solvent vapor and heat treatment the N-substitution PUs exhibit surface wetting reversibility behavior.

EXPERIMENTAL

Materials

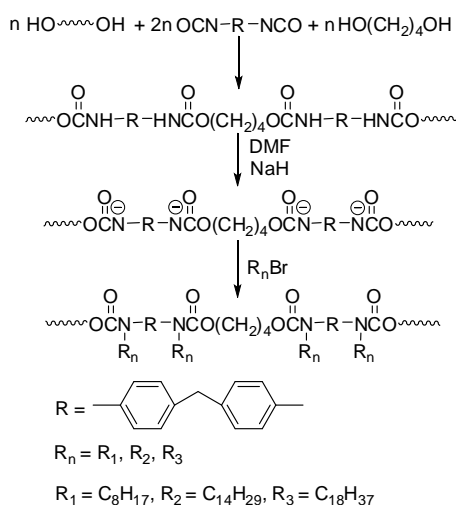
Dimethylformamide (DMF) was distilled fractionally over CaH₂ under reduced pressure and stored over molecular sieves of 4 Å. 4,4'-methylene-bis(phenylisocyanate) (MDI), polypropylene glycol (PPG, Mn = 1000), 1,4-butanediol (1,4-BDO), 1-Bromooctane (C₈H₁₇Br), 1-Bromotetradecane (C₁₄H₂₉Br), 1-Bromooctadecane (C₁₈H₃₇Br) and sodium hydride (NaH, 60% suspension in mineral oil) were purchased from Aladdin Chemistry Co. Ltd and used as received. Methanol, ethyl acetate and n-hexane were used without further purification.

Preparation of PU

Polypropylene glycol (PPG, $M_n = 1000$) in DMF was added to 4,4'-methylene-bis(phenylisocyanate) (MDI) solutions in DMF in a three-necked, round-bottom flask under argon atmosphere. The polymerization was carried out at 70-80 °C for 4 h. The reaction was detected by in-situ FTIR and the completion of prepolymer formation was confirmed by half of the intensity of NCO group. After preparation of isocyanate-terminated prepolymer, stoichiometric 1,4-butanediol (BDO) dissolved in DMF as a chain extender was added. The reaction was continued for 6 h at 70-80 °C. The PU was synthesized based on the molar ratio MDI/PPG/BDO = 2:1:1. The resulting polymers were precipitated in excess water, filtered, then washed with methanol and precipitated in excess water to remove low molecular weight materials. To further purify the obtained polymers, they were washed with deionized water and dried in a vacuum at 70 °C.

Preparation of *N*-alkyl-substituted PU

A sample of the PU, dissolved in dried DMF, was placed in a three-necked flask. Stoichiometric NaH (the molar ratio NaH/CNO = 1:1) was added into the stirred polymer solution in the reactor under argon atmosphere. The reaction mixture was kept at a temperature not exceeding 0 °C in a cryogenic thermostat. After the evolution of H₂ ceased, the appropriate amount of bromoalkane (C₈H₁₇Br, C₁₄H₂₉Br, C₁₈H₃₇Br) was added, and the mixture was reacted for some time at certain temperature (the reaction time and temperature will be described in the section of degree of substitution). Followed by removal of DMF by vacuum distillation, the reaction mixture was chromatographed on a silica gel (ethyl acetate/*n*-hexane = 1/3) to afford the purified polymers. The *N*-octyl-substituted polyurethane, *N*-tetradecyl-substituted polyurethane and *N*-octadecyl-substituted polyurethane are abbreviated to PU-C₈, PU-C₁₄, PU-C₁₈, respectively in this work. The synthetic routes and chemical structures of the PU and *N*-substituted PU are shown in Scheme 1.



Scheme 1 The preparation of *N*-alkyl-substituted polyurethanes.

Measurements

Nuclear Magnetic Resonance Spectroscopy

¹H-NMR spectra of the polymers dissolved in DMSO-d₆ or CDCl₃ were recorded at the ambient temperature with a ¹H-NMR spectrometer (Bruker AVANCE II 400). Chemical shifts (δ) were given in parts per million with tetramethylsilane (TMS, δ = 0 ppm) as a standard.

Fourier Transform Infrared Spectroscopy

Fourier transform infrared (FT-IR) spectra were performed on an IR Prestige-21 FTIR Spectrometer (Shimadzu, Japan) at room temperature. All IR spectra covered in the range of 400-4000 cm⁻¹. N-substituted PU was cast onto a KBr plate for analysis.

Differential Scanning Calorimetry

Differential Scanning Calorimetry (DSC) was examined with a TAQ-10 DSC instrument. The sample films were cut and weighed from 5 to 10 mg. Samples were first heated from -80 °C to 120 °C and cooled to -80 °C at 15 °C /min, and then reheated to 120 °C at 15 °C /min under the nitrogen atmosphere with a flow rate of 40 mL/min. Data reported herein were taken from the second heating cycle and were analyzed using TA universal analysis software.

X-ray Diffraction

X-ray diffraction (XRD) analyses of the polymers were carried out on a D8- ADVANCE X-ray diffractometer (Bruker AXS, Germany) with Cu-Kα radiation (λ = 1.5406 Å) at room temperature. The 2θ angle was ranged from 3 to 70°.

Atomic Force Microscopy

Surface morphology of the N-alkyl-substituted polyurethanes films was observed by Multimode 8 Nanoscope V system atomic force microscopy (Bruker, America) in tapping mode. The films were prepared by spin-coating (spin speed of 1500 rpm and spin time of 30 s) the N-substituted PU solutions onto silicon wafers at room temperature and then dried in vacuum at ambient temperature for 24 h to evaporate the residual solvent. Prior to spin-coating, the silicon wafers were treated with hot piranha solution (70:30 v/v, 98% H₂SO₄/30% H₂O₂) for 2 h, and were rinsed with large amounts of deionized water several times and dried.^{29,30}

Scanning Electron Microscopy

The morphologies of the N-substituted polyurethane films were characterized by scanning electron microscopy (SEM, QUANTA 200), operating at 20 kV. The samples were fixed to an aluminum holder with a double-sided adhesive film and were then coated with a thin layer of gold.

Water Contact Angle Measurement

The static contact angles were measured on a JC2000C1 (Shanghai, China) contact angle system at ambient temperature. Deionized water droplets (about 6 μL) were dropped carefully onto the films. The average contact angle value was obtained by measuring at five different

positions of the same sample.

RESULTS AND DISCUSSION

Synthesis

N-substituted polyurethanes were synthesized by a two-step reaction from polyurethane, as depicted in Scheme 1. In the first step, sodium hydride generates the active anion sites on the polyurethane back bone. The mixture was allowed to react for about 1 h. In the second step, the prepared urethane polyanion acting as a nucleophile reacts with bromoalkane to prepare N-substituted PU. Sodium hydride (NaH)/dimethylformamide (DMF) is used as an alkali/solvent in the N-substitution process of PU.

The singlet N-H proton peak was observed at 9.49 ppm for PU (Fig.1a); however, in the spectra of the fully N-substituted PU, the signal of the urethane proton (NH-COO) virtually disappeared as expected (Fig.1b). In the case of N-substituted PU, a new peak was observed at 0.88 ppm assigned to protons of the newly formed COO-N-(CH₂)₁₇-CH₃ (Fig.1b), which is the end group of the substituent. Also the signals due to the protons of phenyl rings in PU appear at 7.07 and 7.33 ppm shifted to 7.14 ppm (Fig.1b) when the nitrogen is alkylated. The disappearance of a signal of the NH proton, the presence of signal of end methyl of substituent and the change of signal of aromatic protons are proof of N-alkylation of the PUs, similar to the N-substituted PEO-PU.²⁵

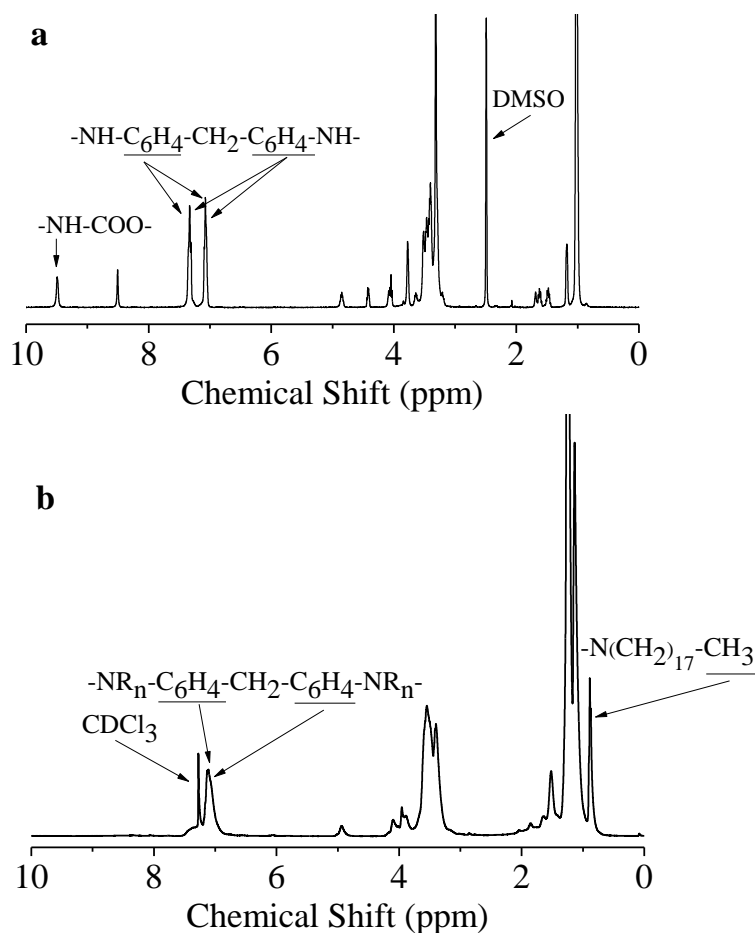


Figure 1 ^1H NMR spectra of PU (a) and PU- C_{18} (b).

FTIR spectroscopic analysis has also been used to confirm the grafting of alkyl with PU. Figure 2a represents the FTIR spectra of PU and PU- C_{18} , which shows N-H stretching around 3300 cm^{-1} obviously decreased and aliphatic C-H stretching at $2850\text{--}3000\text{ cm}^{-1}$ increased by N-substitution. The hydrogen-bonding characteristics of the hard-segment urethane carbonyl groups at 1600 cm^{-1} for bonded groups and 1640 cm^{-1} and 1725 cm^{-1} for free groups in spectra of PU, while 1600 cm^{-1} for bonded groups, 1660 cm^{-1} and 1700 cm^{-1} for free groups in spectra of PU- C_{18} as shown in Fig. 2b. Compared with PU, the intensity of the bonded carbonyl (C=O) and N-H absorption of PU- C_{18} decreased while the free carbonyl (C=O) absorption of PU- C_{18} increased due to the N-alkyl-substituted PU diminished hydrogen bonds formation.²⁶

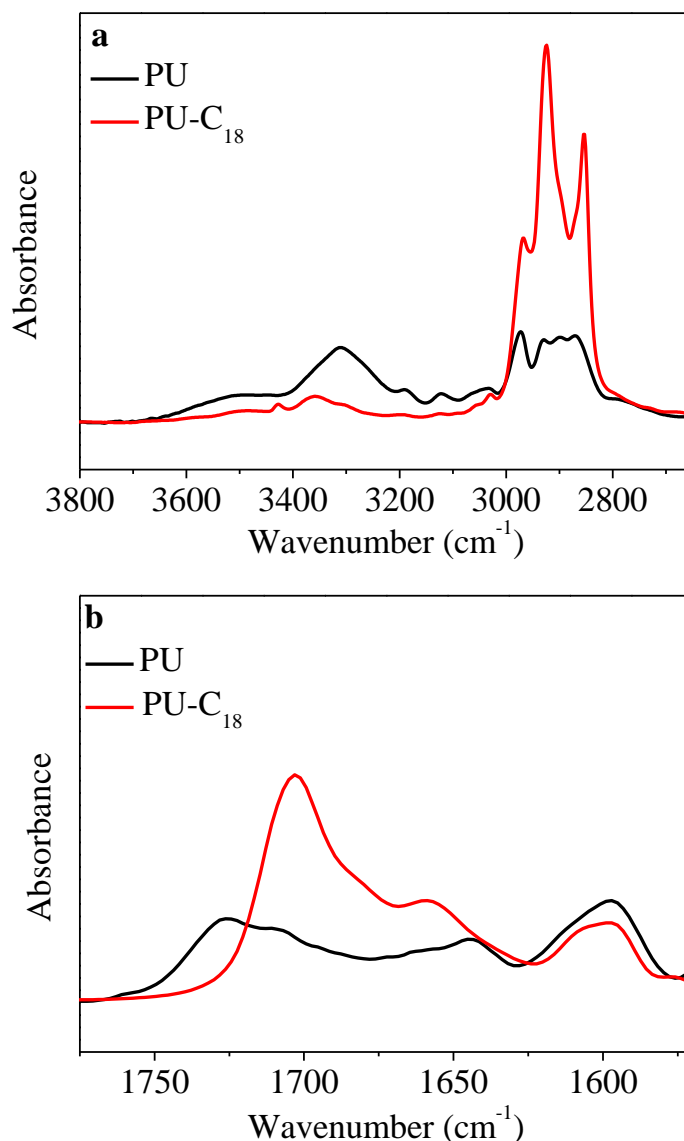


Figure 2 IR spectra before and after N-modification of polyurethane (PU and PU-C₁₈).

Degree of Substitution

To investigate the ideal grafting conditions for N-substitution, the comparative experiments were applied to obtain the ideal reaction time, temperature and material ratio. Aromatic protons of MDI moiety in polyurethane are not changed before and after the N-substitution reaction of polyurethane and can be used as the internal standard for the determination of the degree of substitution. The following formula (1-1) was used to calculate the degree of substitution.

$$DS = (4b/3a) \times 100\% \quad (1-1)$$

DS is the abbreviation of degree of substitution; a and b are the number of aromatic proton

and end methyl proton of substituent in ^1H -NMR spectra of N-substituted PU, respectively.

Reaction temperature, reaction time and material ratio of $\text{C}_8\text{H}_{17}\text{Br}$ and CNO have significant influence on the degree of substitution and were taken as three factors. All the experiment values were shown in Table 1 and Figure 3. The values of degree of substitution in Table 1 are calculated by formula (1-1).

Table 1 Degree of substitution of N-substitution of PU at different reaction conditions.

NO.	Reaction Temperature (°C)	Reaction Time (h)	Material Ratio n (RBr/CNO)	Substitution Degree (%)
1	60	0.5	1	78.17
2	60	1	1	84.67
3	60	2	1	90.17
4	60	4	1	90.17
5	60	6	1	90
6	20	2	1	81.17
7	40	2	1	85.83
8	70	2	1	90
9	80	2	1	90.17
10	60	2	0.5	49.67
11	60	2	1.5	96.67
12	60	2	2	97.17
13	60	2	3	97.17

Figure 3a shows that degree of substitution gradually increased with increasing the reaction time and reached a maximum degree of substitution with the reaction time of 2 h. Further increase in the reaction time does not result in the increase of the degree of substitution meaning that the reaction reached an equilibrium. The degree of substitution gradually increased with increasing the reaction temperature and did not increase when reaction temperature exceeded 60 °C (Fig. 3b). Figure 3c implies that degree of substitution gradually increased with increasing material ratio and a plateau appeared when material ratio of $\text{C}_8\text{H}_{17}\text{Br}$ and CNO was 2:1. Summarizing all the results above, we can draw a conclusion that PU- C_8 has a maximum degree of substitution with the reaction time of 2 h, the reaction temperature of 60 °C and material ratio ($\text{C}_8\text{H}_{17}\text{Br}/\text{CNO}$) of 2:1.

In the N-substitution of PU, the overall reaction under the NaH/DMF condition was nearly completed within 3 h, determined by the above analysis. Figure 3d shows the influence of substituent on degree of substitution of N-substituted PUs which was synthesized at the experiment conditions ($t = 2\text{h}$, $T = 60\text{ }^\circ\text{C}$, $n(\text{RBr}/\text{CNO}) = 3:1$). The degree of substitution gradually decreased with increasing the chain length of substituent. The generation of N-substitution of PU in the alkali environment involves a nucleophilic attack on one carbon of the bromoalkane and the reaction rates critically depend on the steric hindrance at the reactive site.³¹ In our case the reaction ability markedly decreased with the increase of the steric

hindrance, resulted from the increased chain length of substituent. .

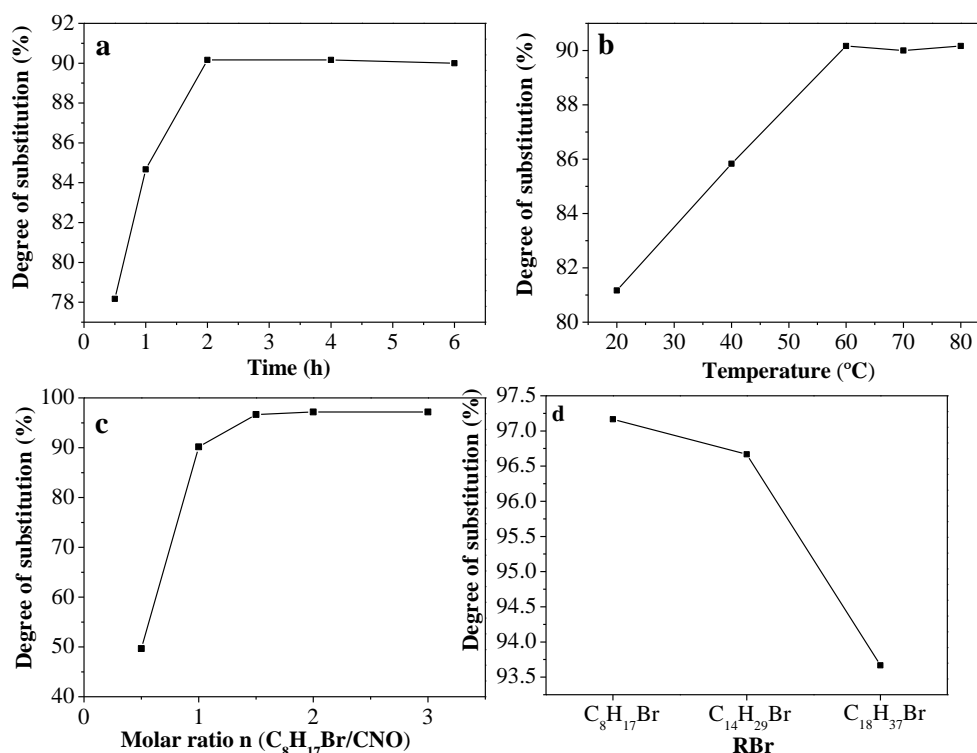


Figure 3 Degree of substitution-reaction conditions curves of N-substituted PUs, (a): DS-Time curve of PU- C_8 , $T = 60\text{ }^{\circ}\text{C}$, $n(C_8Br/CNO) = 1:1$; (b): DS-Temperature curve of PU- C_8 , $t = 2\text{ h}$, $n(C_8Br/CNO) = 1:1$; (c): DS-Material Ratio curve of PU- C_8 , $t = 2\text{ h}$, $T = 60\text{ }^{\circ}\text{C}$; (d): DS-RBr curve of N-substituted PUs (PU- C_8 , PU- C_{14} and PU- C_{18}), $t = 2\text{ h}$, $T = 60\text{ }^{\circ}\text{C}$, $n(RBr/CNO) = 3:1$.

Properties of N-substituted PUs

Thermal Behaviors

The thermal properties of the N-substituted PUs were investigated by DSC measurement as shown in Figure 4. Compared with PU, which shows that the glass transition temperature is $-6\text{ }^{\circ}\text{C}$, all the N-substituted PUs revealed reduced glass transition temperature (T_g). The hydrogen bonding of the urethane between NH and C=O restricts the segmental motion of the chain. Also, N-substitutions reduce the extent of hydrogen bonds formation, resulted in the increase of the chain flexibility, which led to a larger gain in entropy on passing from the glass-like state into the melt, and in turn caused a decreasing glass transition temperature.³²

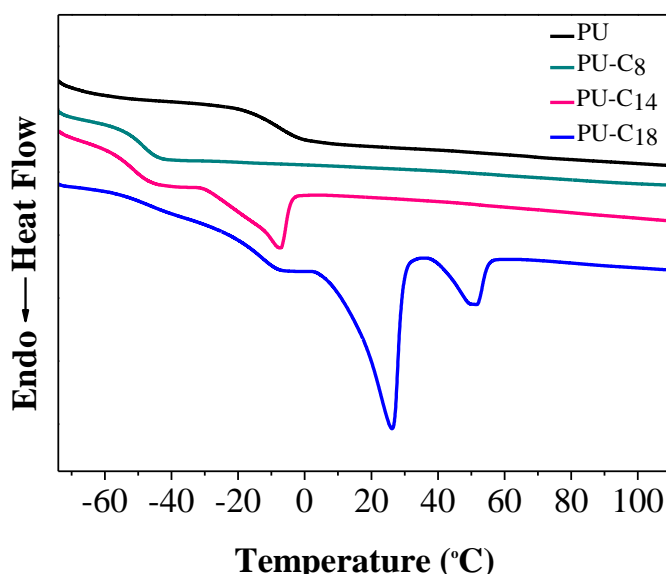


Figure 4 DSC thermograms of original PU and N-substituted PUs.

For all N-substituted PUs, the glass transition temperature is increased with increasing the chain length of substituent. This may be due to that the extent of hydrogen bonds formation of N-substituted PU was in order of $PU-C_8 < PU-C_{14} < PU-C_{18}$, which resulted by that the degree of substitution decreased as the alkyl chain length increased as described above. $PU-C_{14}$ and $PU-C_{18}$ also revealed the melting point (T_c) at $-7^\circ C$ and $26^\circ C$, respectively. The two values should be assigned to T_c of alkyl chain of $C_{14}H_{29}$ - and $C_{18}H_{37}$ -, similar to T_c of tetradecane and octadecane at $5.9^\circ C$ and $28.2^\circ C$, respectively. For $PU-C_{18}$, another T_c value observed at $51^\circ C$, was assigned to the characteristic of $PU-C_{18}$ polymer. Compared with the melting temperature of $PU-C_{18}$, there was no T_c of $PU-C_8$ and $PU-C_{14}$, which was in accordance with their physical states (The physical state of $PU-C_8$, $PU-C_{14}$ and $PU-C_{18}$ was liquid, liquid and solid, respectively.) at room temperature.

XRD Analysis

To confirm the crystalline nature of the N-substituted PUs, X-ray diffraction (XRD) measurement was carried out on these samples and their corresponding XRD patterns are given in Figure 5. The spectrum of $PU-C_{18}$ shows that three diffraction peaks are located at $2\theta = 6^\circ$, 21° and 42° , indicating the crystallinity of $PU-C_{18}$, agreed well with results detected by DSC measurements. For $PU-C_8$ and $PU-C_{14}$, more amorphous structures were obtained, as shown by the presence of one peak in the diffraction pattern (Fig.5). There was no characteristic crystal diffraction peak of $PU-C_{14}$, which may be attributed to the weak crystalline of sample.

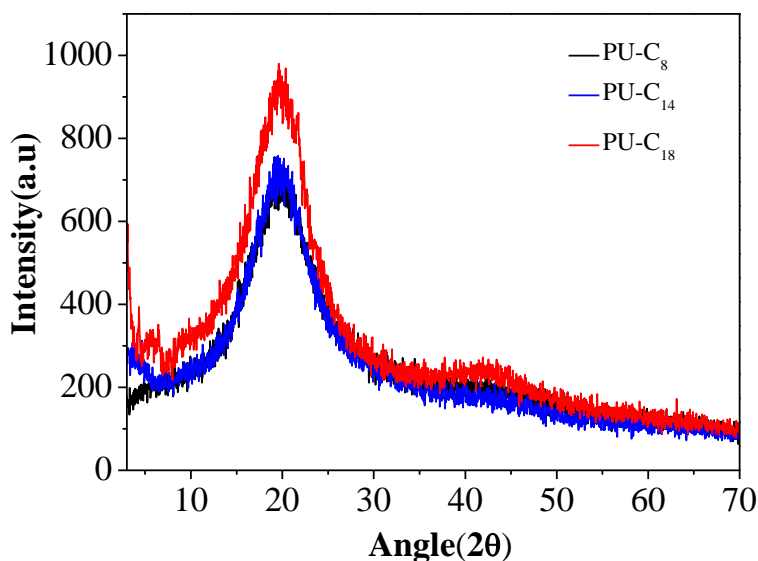


Figure 5 XRD patterns of N-substituted PUs.

Surface Morphology (AFM)

The assumption based on DSC and X-ray analysis, that is, the presence of amorphous structure of PU-C₈ and microphase separation of PU-C₁₄ and PU-C₁₈, is supported by atomic force microscopy (AFM) (Fig.6). Thin films were prepared by spin-coating the homogeneous and transparent polymer/DMF solution. Representative AFM images of PU-C₈ shows an island amorphous structure and the area of island increased with increasing the concentration (Fig.6a-a''). For PU-C₁₄, a microphase-separated nanostructure, with hard segments (nanofiber-like) embedded into an amorphous PPG soft segments, were clearly observed (Fig. 6b-b''). A more densely packed fiber-like structure was observed for PU-C₁₈, due to its higher crystalline nature compared to PU-C₁₄, as confirmed by DSC and XRD (Fig. 6c-c'').

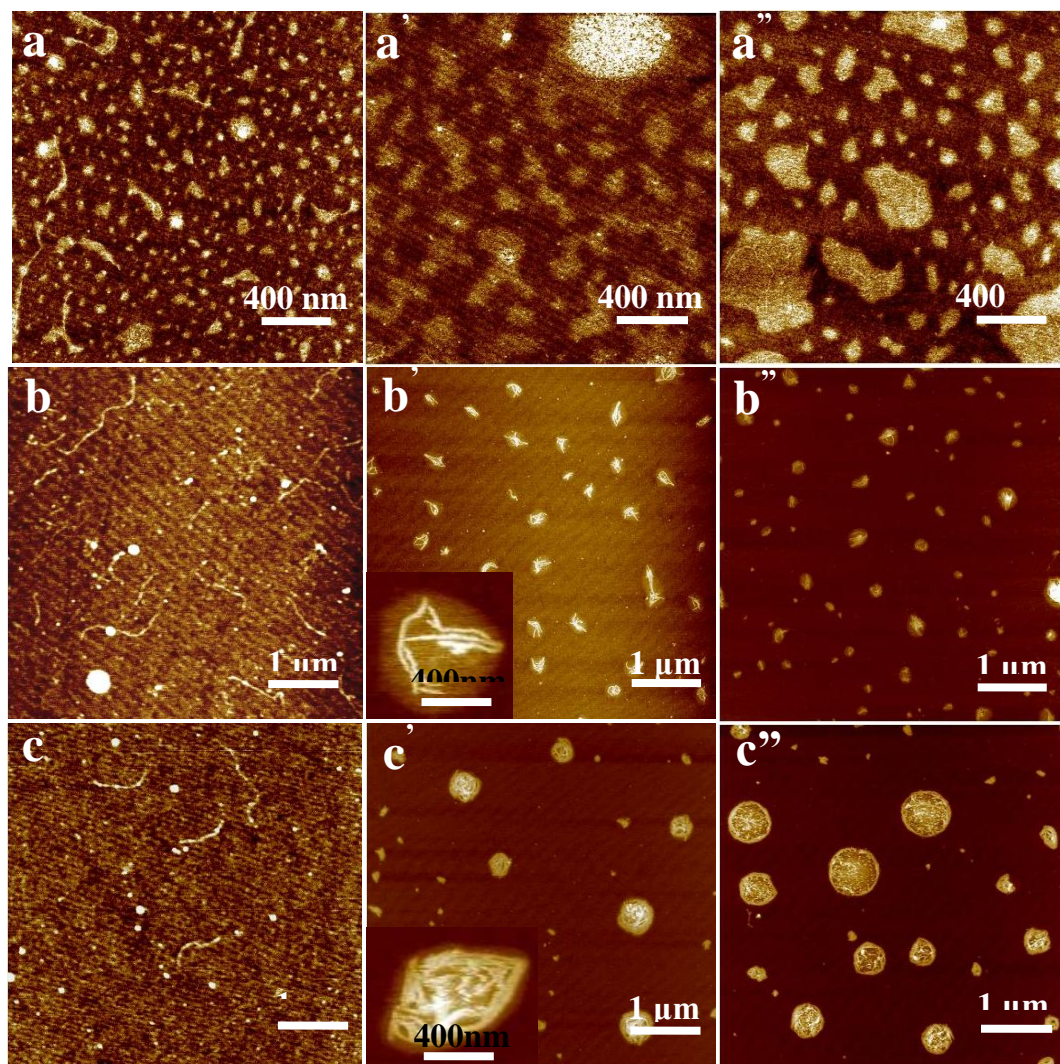


Figure 6 The AFM height images of PU-C₈ (a, a', a''), PU-C₁₄ (b, b', b'') and PU-C₁₈ (c, c', c'') at the concentration of 0.1 mg/ml (a, b, c), 0.5 mg/ml (a', b', c') and 1.0 mg/ml (a'', b'', c''), respectively. DMF was used as solvent.

To check the effect of solvent evaporation rate on the film morphology, we use CHCl₃ as the solvent which has a much low boiling point (61 °C) compared to DMF (153 °C). For PU-C₁₄ and PU-C₁₈, rod-like morphologies are evidently dispersed in larger and more clearly separated domains of the other phase, similar to the morphology of the film by using DMF as solvent (Fig.7b-b'' and Fig.7c-c''). For PU-C₈, the samples also revealed rod-like morphology embedded in polymer matrix (Fig.7a-a'') due to a fast evaporation rate process. The increase in the evaporation rate induces an increase in the temperature gradient and the film equilibrates slower than the heat loss by the evaporation process, resulted in a microphase separation system.³³ In addition, hydrophobic interactions of the alkyl chains are responsible for the hard-rod like morphology formation.

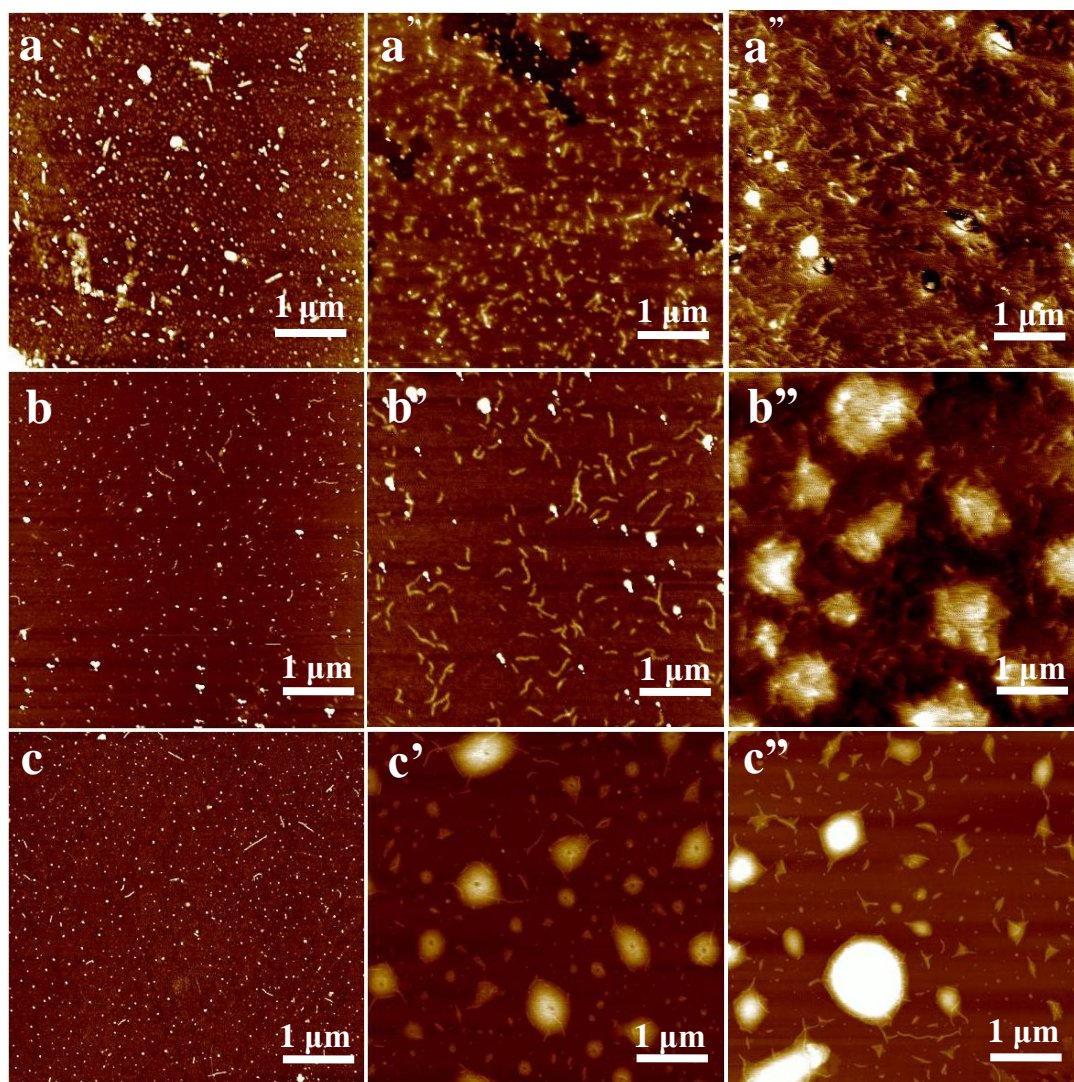


Figure 7 The AFM height images of PU-C₈ (a, a', a''), PU-C₁₄ (b, b', b'') and PU-C₁₈ (c, c', c'') at the concentration of 0.1 mg/ml (a, b, c), 0.5 mg/ml (a', b', c') and 1.0 mg/ml (a'', b'', c''), respectively. CHCl₃ was used as solvent.

Stimuli-Responsive Behavior of the Films

To investigate the surface wetting properties of the synthesized N-substituted PUs, the static contact angles were measured by adding a droplet of water on the thin polymer films. The casting films were made by dropping the polymer solutions onto the glass slides and dried in a vacuum oven at room temperature. The measurements revealed that the water contact angle of PU-C₈, PU-C₁₄ and PU-C₁₈ was $81 \pm 2^\circ$, $88 \pm 2^\circ$ and $92 \pm 2^\circ$, respectively (Table 2). It is reasonable that the increased contact angle along with increasing the chain length of substitution due to the hydrophobic character of alkyl chains.

To study the stimuli-responsive behavior of the N-substituted PUs films, a nonpolar solvent n-hexane was used to induce the structural surface reorganization. Solvent vapor

annealing has been carried out using a simple experimental system in which N-substituted PUs films are placed in a chamber containing a reservoir of n-hexane (a good solvent for alkyl chains but a nonsolvent for N-substituted PUs), whose evaporation provides a solvent vapor environment. The films were annealed for 12 h and dried in a vacuum oven at room temperature.

The water contact angle of PU-C₈, PU-C₁₄ and PU-C₁₈ after being underwent solvent vapor annealing was 91±2°, 106±2° and 113±2°, respectively. The results show that the contact angle increased significantly compared with the same N-substituted PU that without being underwent solvent vapor annealing. During the course of exposure to n-hexane vapor, the mobility of alkyl chain of N-substituted PU is increased, which resulted in a structural surface reorganization and most of the alkyl chains are moved to out-most surface of the films.

Table 2 Contact angles of N-substituted PUs before and after solvent treatment

Samples	DS (%)	CA ^a (°)	CA ^b (°)
PU-C ₈	97.17	81±2	91±2
PU-C ₁₄	96.67	88±2	106±2
PU-C ₁₈	93.67	92±2	113±2

^aWithout solvent vapor annealing.

^bAfter solvent vapor annealing.

Scanning electron microscopy (SEM) was also performed to characterize the surface morphology. Figure 8 shows representative SEM images of PU-C₁₈ films before and after solvent vapor annealing. Microphase separated rod-like structures are observed in the full coverage of the films (Fig. 8a). After the n-hexane treatment the rod-like hard segments of the PU-C₁₈ become more clear and seem to stand on the soft matrix (Fig. 8b). The hydrophobic alkyl chains are believed to be the contribution of the increased water contact angle of the films after the solvent vapor annealing.

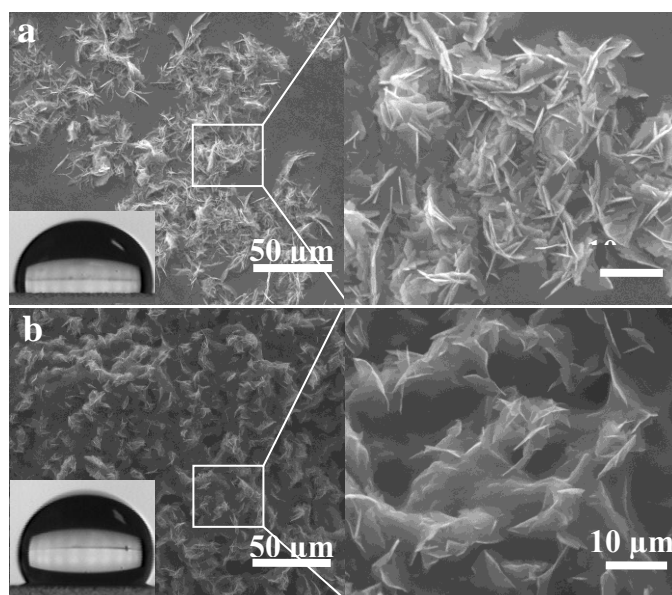


Figure 8 SEM images of PU-C₁₈ before (a) and after (b) solvent vapor annealing (insets show sessile water droplet on the films).

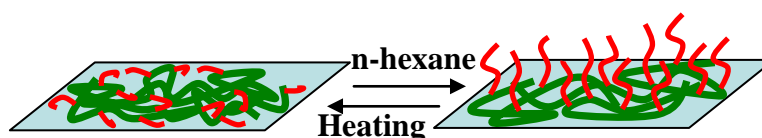


Figure 9 Schematic plot of PU-C₁₈ films by solvent and heat treatment (polymer backbone is drawn in green, alkyl chain in red).

To increase the chain mobility, the samples (e.g. PU-C₁₈) which underwent hexane solvent treatment, were kept at 55 °C just above the melting point of PU-C₁₈ detected by DSC for 4 h. Water contact angle revealed that the surface wetting properties come back to the initial state with $\theta = 92^\circ$ (Fig. 9). High temperature increases the chains movement, resulted in a regression of the films similar to the initial state. Solvent and heat treatment of films reveal the adaptive properties and the stimuli-responsive character of the N-alkyl-substitution PU, with observed contact angle shifts of up to 21°.

CONCLUSIONS

In summary, N-substituted PUs (PU-C₈, PU-C₁₄ and PU-C₁₈) with different alkyl chain length were successively synthesized by metalation of PU prepared from MDI, PPG, and BDO in DMF, and then the treatment of the obtained urethane polyanion with bromoalkane. ¹HNMR analysis revealed that high-substitute degree of PU-C₈ was obtained when the N-substitution reaction operated at 60 °C for 2 h, with the molar ratio of C₈H₁₇Br and CNO of

2:1 and the degree of substitution gradually decreased with increasing the chain length of substituent. DSC revealed that T_g of the N-substitution PU decreased by comparing with original PU and increased with increasing chain length of substituent. Microphase-separated nanostructure, with hard segments (nanofiber-like) embedded into an amorphous PPG soft segments, are revealed by AFM. Reversible stimuli-responsive surface wetting behavior was observed by contact angle measurements. By keeping the samples undergoing solvent vapor annealing, hydrophobicity is increased with increasing the chain length of the substituent, which was due to that alkyl chains move to out-most surface of the films. By heating the solvent treated films above the melting points, the surface wetting properties come back to its initial state. This reversible reorganization of the polymer film is promising for applications for surfaces with controlled release, self-cleaning, and self-refreshing abilities³⁴⁻³⁶.

ACKNOWLEDGMENT

The financial supported by Program for Scientific Research Innovation Team in Colleges and Universities of Shandong Province, the National Natural Science Foundation of China (21204044, 21176147 and 21276149), Shangdong Outstanding Young Scientist Award Fund (BS2012CL028) and Ji'nan Overseas Students Pioneer Plan (20120202) are gratefully acknowledged.

REFERENCES AND NOTES

- 1 Y. Lee, S. Fukushima, Y. Bae, S. Hiki, T. Ishii, K. Kataoka, *J. Am. Chem. Soc.* **2007**, *129*, 5362-5363.
- 2 C. L. Bayer, N. A. Peppas, *J. Control. Release* **2008**, *132*, 216-221.
- 3 A. S. Hoffman, *J. Control. Release* **2008**, *132*, 153-163.
- 4 W. M. Huang, B. Yang, Y. Zhao, Z. Ding, *J. Mater. Chem.* **2010**, *20*, 3367-3381.
- 5 I. Tokareva, S. Minko, J. H. Fendler, E. Hutter, *J. Am. Chem. Soc.* **2004**, *126*, 15950- 15951.
- 6 M. Motornov, R. Sheparovych, R. Lupitsky, E. MacWilliams, S. Minko, *Adv. Mater.* **2008**, *20*, 200-205.
- 7 P. M. Mendes, *Chem. Soc. Rev.* **2008**, *37*, 2512-2529.
- 8 I. Luzinov, S. Minko, V. V. Tsukruk, *Soft Matter* **2008**, *4*, 714-725.
- 9 M. Motornov, S. Minko, K. J. Eichhorn, M. Nitschke, F. Simon, M. Stamm, *Langmuir* **2003**, *19*, 8077-8085.
- 10 M. A. C. Stuart, W. T. S. Huck, J. Genzer, M. Müller, C. Ober, M. Stamm, G. B. Sukhorukov, I. Szleifer, V. V. Tsukruk, M. Urban, F. Winnik, S. Zauscher, I. Luzinov, S. Minko, *Nat. Mater.* **2010**, *9*, 101-113.
- 11 Ph. Game, D. Sage, J. P. Chapel, *Macromolecules* **2002**, *35*, 917-923.

- 12 M. F. Sonnenschein, N. Rondan, B. L. Wendt, J. M. Cox, *J. Polym. Sci., Part A: Polym. Chem.* **2004**, 42, 271-278.
- 13 W. N. Sivak, I. F. Pollack, S. Petoud, W. C. Zamboni, J. Zhang, E. J. Beckman, *Acta Biomater.* **2008**, 4, 1263-1274.
- 14 H. Yeganeh, M. Barikani, F. N. Khodabadi, *Eur. Polym. J.* **2000**, 36, 2207-2211.
- 15 H. C. Beachell, J. C. P. Buck, *J. Polym. Sci., Part A: Polym. Chem.* **1969**, 7, 1873-1879.
- 16 S. Gogolewski, *Colloid Polym. Sci.* **1989**, 267, 757-785.
- 17 D. J. Liaw, S. P. Lin, *Eur. Polym. J.* **1996**, 32, 1377-1380.
- 18 I. S. Alferiev, N. R. Vyavahare, C. X. Song, R. J. Levy, *J. Polym. Sci., Part A: Polym. Chem.* **2001**, 39, 105-116.
- 19 H. C. Beachell, C. P. N. Son, *J. Appl. Polym. Sci.* **1964**, 8, 1089-1096.
- 20 T. L. Cairns, H. D. Foster, A. W. Larchar, A. K. Schneider, R. S. Schreiber, *J. Am. Chem. Soc.* **1949**, 71, 651-655.
- 21 M. Takayanagi, T. Katayose, *J. Polym. Sci., Polym. Chem. Ed.* **1981**, 19, 1133- 1145.
- 22 M. Takayanagi, T. Katayose, *J. Polym. Sci., Polym. Chem. Ed.* **1983**, 21, 31-39.
- 23 H. Sivriev, S. Georgiev, G. Borissov, *Eur. Polym. J.* **1990**, 26, 73-76.
- 24 D. J. Liaw, S. P. Lin, *Macromol. Mater. Eng.* **1996**, 239, 191-199.
- 25 J. O. Kweon, Y. K. Lee, S. T. Noh, *J. Polym. Sci., Part A: Polym. Chem.* **2001**, 39, 4129-4138.
- 26 H. S. Choi, S. T. Noh, *J. Polym. Sci., Part A: Polym. Chem.* **2002**, 40, 4077-4083.
- 27 S. M. S. Mohaghegha, M. Barikania, A. A. Entezami, *Colloids Surf. A: Physicochem. Eng. Aspects* **2006**, 276, 95-99.
- 28 D. J. Liaw, S. P. Lin, *J. Appl. Polym. Sci.* **1996**, 61, 315-319.
- 29 L. B. Liu, H. J. Kim, M. Lee, *Soft Matter* **2011**, 7, 91-95.
- 30 L. B. Liu, D. J. Hong, M. Lee, *Langmuir* **2009**, 25, 5061-5067.
- 31 W. H. Moore, S. Krimm, *Biopolymers* **1976**, 15, 2439-2464.
- 32 B. Espenschied, R. C. Schulz, *Polym. Bull.* **1981**, 5, 489-495.
- 33 L. B. Liu, J. K. Kim, M. Lee, *ChemPhysChem* **2010**, 11, 706-712.
- 34 A. Misra, W. L. Jarrett, M. W. Urban, *Macromolecules* **2007**, 40, 6190-6198.
- 35 D. V. Andreeva, D. Fix, H. Mohwald, D. G. Shchukin, *Adv. Mater.* **2008**, 20, 2789-2794.
- 36 M. W. Urban, *Prog. Polym. Sci.* **2009**, 34, 679-687.